A Study on the Charging and Diagnosis System of xEV Reusable Waste Battery

Sung-Jun Park[1], Chun-Sung Kim[2], Seong-Mi Park[3*]

〈Abstract〉

As the supply of xEV in Korea is rapidly increasing, the amount of waste batteries is expected to increase rapidly, but the current recycling system for waste xEV batteries is very insufficient. In order to properly utilize the xEV reusable battery module, it is essential to classify it into a type that has similar discharge characteristics to the current state of health(SOH), which is the discharge capacity of the battery. This paper proposes a system that can minimize the exchange of energy with the KEPCO system by using the charging/discharging method by circulating power between batteries in order to minimize the power consumption when charging and discharging waste batteries. In the proposed system, a function to measure parameters during the charging/discharging test of the waste battery was implemented to build a customized big date for the test waste battery. In addition, the dynamic characteristics of the proposed circuit were analyzed using PSIM, which is useful for power electronics analysis, and the validity of the proposed circuit was verified through experiments.

Keywords : xEV Reusable Waste Batteries, Charging/Discharging Method, State Of Health(SOH), Direct Current Internal Resistance(DCIR), Alternating Current Internal Resistance(ACIR)

1 Main Author, Dept. of Electrical Engineering, Chonnam National University, Professor
E-mail: sjpark1@jnu.ac.kr
2 Author, Green Energy Institute, Team leader
E-mail: minisung13@gei.re.kr
3* Corresponding Author, Dept. of Lift Engineering, Korea Lift College, Associate Professor
E-mail: seongmi@klc.ac.kr

1. Introduction

As the domestic xEV supply plan rapidly increases to 350,000 units in 2022, the amount of waste batteries is expected to increase rapidly. However, the current recycling system for waste xEV batteries is very insufficient. According to Article 26 of the 「Act on Resource Circulation of Electrical/Electronic Products and Automobiles」, scrapped vehicles are to be recycled according to the recycling methods and standards prescribed by Presidential Decree. However, detailed recycling methods for waste batteries of electric vehicles have not yet been prepared. Battery end of life(EOL) minimum discharge capacity rate is generally defined as 80 [%] of rated capacity, which is a capacity that does not pose a risk to vehicle operation in the case of automobiles, and 70 [%] of rated capacity in case of energy storage system(ESS) is used[1]-[3]. In order to properly utilize such an xEV reusable battery module, it is essential to classify it into a type having similar discharge characteristics to the state of health(SOH), which is the discharge capacity of the battery. In order to classify battery characteristics for a short period of time or without completely charging and discharging the battery, studies on direct current internal resistance(DCIR) and aternating current internal resistance(ACIR), which are internal parameter estimation methods, are being actively conducted[4]-[6]. However, although this method accurately estimates the parameters of the battery, there is a disadvantage that it is possible to have big data about the battery in order to estimate the SOH. In addition, as various voltages and capacities of batteries currently used in the industry are mixed, there will be waste batteries of various products in the future, and it is impossible to build big data for these batteries, so there is a limit to responding to this[7]-[8].

Currently, the most reliable method for the classification of waste batteries is to perform full charge/discharge of the battery and use the charging/discharging characteristic curve of the battery. However, the cost of constructing a large number of high-efficiency two-way charging and discharging systems is a major obstacle. Therefore, the demand for an economical system that can minimize power consumption while performing charge and discharge tests on a large number of waste batteries is rapidly increasing[9]-[10].

This paper proposes a system that can minimize the exchange of energy with the KEPCO system by using the charging and discharging method by circulating power between batteries in order to minimize the power consumption when charging and discharging waste batteries. The proposed system is a customized big date for test waste batteries was built by implementing a function that can measure parameters during the charging/discharging test of waste batteries. In addition, we proposed a series of internal resistance normalized similarity functions suitable for classification of recycled batteries. Experiments were conducted to validate the proposed system and reusable battery classification.

2. Battery Characterization

2.1 Battery Equivalent Circuit through EIC Method

Electrochemical Impedance Spectroscopy(EIS) is widely used in general industry because it is easy to understand the equivalent circuit for impedance measurement principle, EIS analysis method, impedance trajectory, Warburg impedance, AC impedance analysis, electrochemical impedance and data analysis, etc..

As shown in Fig. 1, the commonly used Randles model is the battery's series-connected electrolyte resistance Ri, parallel-connected charge double layers Cd, charge transfer resistance Rd and diffusion Zw representing the impedance by inductive reaction. It is represented by equalizing it with an electric circuit. This modeling, along with electrochemical impedance spectroscopy, is mainly used in a form that can be analyzed by equating the characteristics of each internal element of the battery to the composition of the electrochemical reaction.

In Randles model, the new equivalent resistance and diffusion model by integrating the voltage source, internal resistance, and

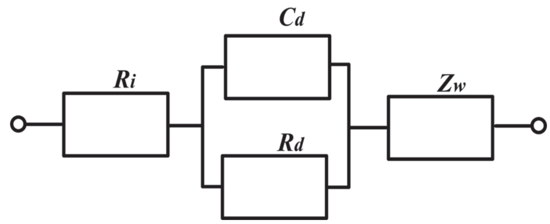

Fig. 1 Composition of battery equivalent circuit

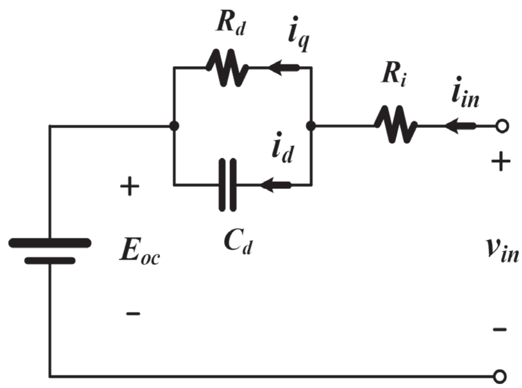

Fig. 2 Simplified battery model

charge transfer resistance is simplified as an RC parallel circuit, as shown in Fig. 2. When the state of charge(SOC) of the battery is high, it is the charge transfer resistance, which is the main resistance of the electro-chemical reaction, and when it is low, the state of the battery can be diagnosed using the diffusion resistance characteristic, which is the main resistance. The charge transfer resistance Ri refers to a potential loss that occurs when a charge generated through a chemical reaction at the battery electrode is transferred to the outside of the battery. The diffusion resistance Rd is equivalent to the electro-chemical reaction occurring on the electrode surface. In the DCIR measurement method, which is a method of estimating battery parameters using

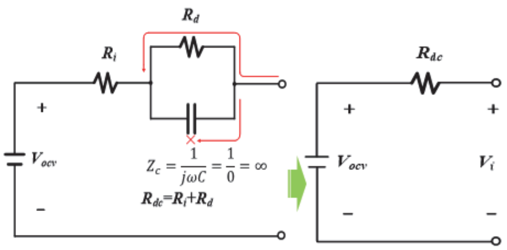

Fig. 3 2-level current parameter equivalent circuit

two-level current and voltage, in the battery equivalent model, the capacitance stage is short-circuited due to the capacitance Cd component at the initial stage of discharging and operates only with the resistor Ri, and the capacitance is opened in the steady state of a constant current. As can be seen, it operates as the sum of the resistors Ri and Rd, and Cd can be calculated from the time constant. Therefore, the necessary information for battery modeling during constant current charging can be solved only by the sum of the internal voltage and resistances Ri and Rd.

Battery internal voltage V_{OCV} and SOC have a linear relationship with each other, and the equivalent circuit for estimating internal voltage during constant current charging can be used as a simplified model as shown in Fig. 3.

In Fig. 3 the internal equivalent resistance R_{DC} of the battery is the sum of the resistances Ri and Rd of the simplified Randles model.

$$R_{DC} = R_i + R_d \tag{1}$$

The internal equivalent resistance is the resistance value for the DC component. In order to estimate the internal voltage of the battery in the charging mode, only the information about Rt can be used to calculate the internal voltage value by detecting the terminal voltage and current. If in 2-level constant current mode, R_{DC} for each terminal voltage and current is defined as follows.

$$R_{DC} = \frac{V_1 - V_2}{I_1 - I_2} \tag{2}$$

In the 2-level constant current charging mode, level 1 is the same as the existing constant current charging, level 2 is a mode added to follow the parameters of the battery in real time, and the internal voltage of the battery is defined as Equation (3)

$$V_{ocv} = V_1 - R_{DC} I_1 = V_2 - R_{DC} I_2 \tag{3}$$

2.2 Reusable Life Battery Life Characteristics

The secondary battery sometimes loses its function as a secondary battery due to abnormal use such as overdischarge or overcharge, but the capacity, which is the ability to store electrical energy, even when used normally, gradually decreases according to the number of charging and discharging. As a result, in order to meet the intended use, it is used until it loses the minimum function required as a secondary battery according to the intended use, and when the minimum function is lost, it is replaced with a new secondary battery and used.

Typically, in the case of EVs, when the capacity of the secondary battery decreases to 80% to 50% of the initial capacity, it is replaced. Secondary batteries for EVs are generally more expensive than lead-acid batteries, and these replaced secondary batteries often have electrical energy storage capacity that is suitable for use in other applications, even if they do not meet their intended use.

Therefore, rather than disposing of the replaced secondary battery from the electric vehicle because it is not suitable for use in an electric vehicle, the method of recycling/reusing the replaced secondary battery for other applications that requires as much energy storage capacity as the energy storage capacity of the electric vehicle In addition to avoiding waste, it is possible to reduce the manufacturing cost of electric vehicles and other devices, and the like. In order to solve the problem of clearly predicting the reuse life in an environment where battery reuse is required, not only the remaining capacity of the battery but also the power life should be considered. For the purpose of calculating the reuse life of a battery, it is necessary to define a definition of calculating the reuse life State Of Reuse(SOR) using the capacity life SOH and the power life state of power(SOP).

Therefore, in the battery reuse life diagnosis method, the SOR means a life that can be reused when a battery that is no longer in use is diagnosed and graded and reused according to its purpose.. In the battery reuse life diagnosis method, SOR is not simply determined by either SOH or SOP, but is determined by establishing a certain relationship between SOH and SOP.

$$SOR = a \times SOH + b \times SOP \quad (4)$$

It corresponds to $0 \leq a \leq 1, 0 \leq b \leq 1$ and $a + b = 1$ in the above equation, and in the battery reuse life diagnosis method, the power life SOP is defined by the following equation.

$$SOP = \left(\frac{V_o - i_s \times (R_s' + R_p')}{V_o - i_s \times (R_{so} + R_{po})} \right) \times 100 \quad (5)$$

R_{so} : when R_s is SOH 100%, SOC 50%

R_{po} : when R_p is SOH 100%, SOC 50%

R_s' : when R_s is 50% SOH and SOC

R_p' : when R_p is 50% SOH and SOC

i_s : standard c-rate current value

Therefore, the current SOH of the battery is determined by comparing it with the initially measured state value based on the state value that changes according to the use of the battery. The standard for the battery SOH definition is defined by the user because the application fields of the battery are very diverse and the performance standards are very different for each field.

2.3 Analysis of Battery Characteristics Using Cyclic Current

For battery reuse, the reuse life should be

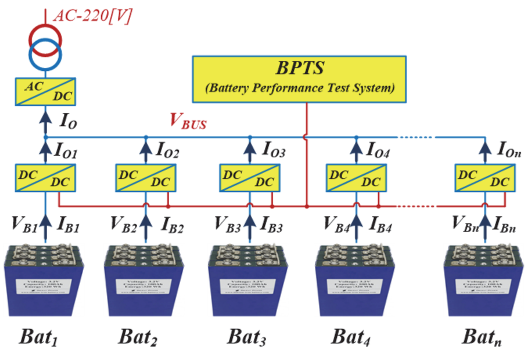

Fig. 4 Charger discharger system using circulating current

defined according to the application environment, and battery packs should be manufactured with the same grade by classifying batteries. A clear way to classify batteries is to perform a full charge/discharge test under defined conditions. When classifying batteries in this way, as shown in Fig. 4, we propose a system that can minimize power consumption for charging and discharging tests.

The proposed system uses a bidirectional DC/DC converter that can transfer energy for each battery to classify multiple waste battery classes and connects to the DC common bus. Each battery is charged and discharged by forming an internal circulating current through the DC bus. At this time, when the total of the internal circulation current becomes zero, the battery charge/discharge test can be performed without external energy supply.

The current to be supplied from the outside in this system is defined as the following equation.

$$I_{ext} = \sum_{k=1}^{n} I_k \qquad (6)$$

The current to be supplied from the outside defined in equation (6) should be supplied from the AC/DC converter, and assuming that the charging and discharging currents are the same, in order to reduce this current, the number of charged and discharged batteries should be the same. A controller operating close to these conditions is managed by the battery performance test system.(BPTS) For waste battery classification, charging and discharging up to SOC 100 [%] by constant current mode and constant voltage mode are possible, but in this case, the battery classification yield is lowered due to prolonged constant voltage charging time. Since it is SOH and SOP that determines the actual battery classification, classification by constant current charging and discharging is sufficient.

Therefore, in this system, constant current and constant voltage charge and discharge are performed on the initial sample battery to analyze the constant voltage charge and discharge characteristics, and in terms of yield increase and ease of circulating current management, battery classification is based on constant current charge and discharge characteristics.

The actual performance of the BPTS is greatly affected by the initial residual capacity of the battery and the time of input. In order to reduce the efficiency of classifying waste batteries and to reduce the external

Table 1. Battery specification sheet

Item	Specifications
Energy(Normal)	822[Wh]
Capacity(Normal)	27.4[Ah]
Voltage	30[V](3.75V/cell)
Battery module configuration	1P8S
Weight	6.5[kg]
xEV Vehicle	LF/JF PHEV

supply current, it is more effective to conduct individual sequential test testers rather than completing multiple test testers at the same time.

When the application environment of the reusable battery is defined, the charge/discharge current is defined, and when the charge/discharge current is defined, the maximum charge/discharge time (Tmax) of each battery is defined. In addition, if the number of DC/DC converters for classification of waste batteries is N, the completion time of one battery tester is determined.

In order to verify the validity of this system configuration method, an experiment was conducted with the reusable battery installed in the xEV shown in Fig. 5. Table 1 shows the battery module specifications. From the battery module specification definition, the range of the reused battery cell's operating voltage is 3 to 4.05 [V], the number of battery cells connected in series is 8, and the minimum voltage is 25V and the maximum voltage is 35 [V]. 5 ~ 95 [%] was reflected.

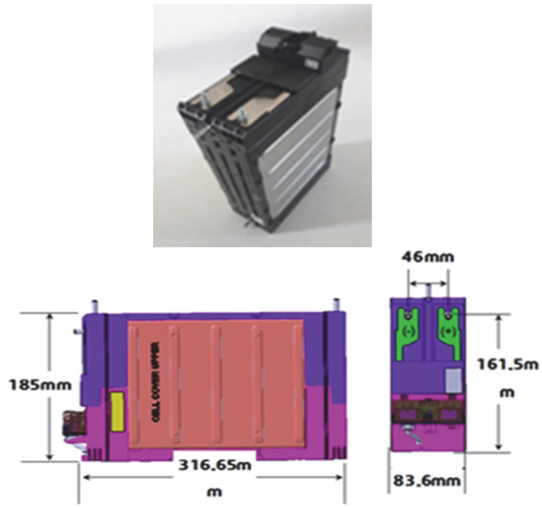

Fig. 5 Li-ion battery modeling and real objects

2.4 Classification of batteries based on similarity

It is desirable to classify reusable batteries into types with similar characteristics and use them. In order to efficiently reuse a battery, when classifying a battery, while the remaining capacity of the battery is similar, the capacity to supply power should also be considered. The remaining capacity of the battery can be easily obtained from the discharge test, but the suitability of the power capacity cannot be easily determined because it differs depending on the operating conditions of the load. The dynamic characteristics of a battery are determined by an internal parameter in the battery equivalent circuit. Therefore, most of the current battery classification is classified as having similar internal parameters.

However, since the internal parameters

appear differently depending on the SOC, the size of the charge/discharge current, and the temperature conditions, the similarity with the behavior of the battery over the entire operating range cannot be confirmed.

Therefore, there is an urgent need for a reuse battery classification technique with similar characteristics under various operating conditions.

Similarity is a measure of how similar two sets of data are, and there are various methods for measuring similarity, such as Mean Squared Difference Similarity, Cosine Similarity, and Pearson Similarity. If data is expressed as a vector on the n dimension, the similarity between the two data may be determined as the distance between the two vectors on the n dimension. The Minkowski distance is a generalization of the Euclidean distance and the Manhattan distance, and is the same as Equation (7).

$$D(x,y) = [\sum_{i=1}^{n} |x_i - y_i|^p]^{1/p} \tag{7}$$

In Equation (7), when p is 1, it is the Manhattan distance and is called the L1 norm, when p is 2, it is the Euclidean distance and is called the L2 norm, and when p is infinity, it is the Chebyshev distance. and is called the L max norm. The cosine similarity is the degree of similarity between the vectors measured using the angle and cosine values between two vectors in the dot product space. The cosine similarity is the similarity with respect to the 'direction'. That

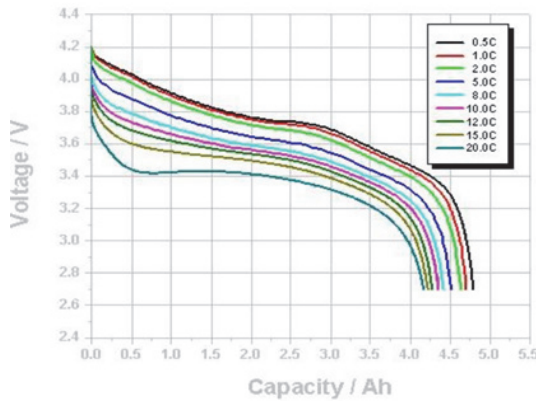

Fig. 6 Discharge characteristics according to discharge current

is, 'distance' is not considered. Here, the difference between Euclidean distance and cosine similarity is that in distance-based similarity, points in close coordinates are measured to have high similarity based on the coordinates, whereas in angle-based similarity, vectors having the same slope and direction are measured to have high similarity.

Fig. 6 shows the terminal voltage characteristics according to the discharge current when the battery is discharged. As can be seen from the figure, the degree of similarity for classification of reusable batteries is mainly determined by the two-dimensional graph data representing the activation of battery parameters, and the definition of similarity of this data needs to be differentiated from the general similarity criteria mentioned above.

In this paper, the degree of similarity of data to understand battery characteristics is defined as Equation (8).

$$S(X,Y)=\sqrt{\frac{1}{N}\sum_{i=1}^{N}[\frac{|x_i-y_i|}{|x_i|+|y_i|}]^2} \qquad (8)$$

The similarity defined in Equation(2-8) is a normalized similarity, and its value ranges from zero to 1, and it can be seen that the smaller the value, the greater the similarity. In the case of reusable batteries, the selection of reference data to be used in the similarity definition of Equation (8) is an important factor. In other words, as data suitable for SOR, which is the re-use life defined in equation (4), in this paper, similarity was evaluated based on the similarity of changes in battery impedance.

3. Proposed System Configuration and Experiment

3.1 Proposal system configuration

Fig. 7 is a system that can measure parameters during the battery charge/discharge test using the cycle power between batteries proposed in this paper.

The proposed system uses a bidirectional DC/DC converter that can transfer energy to and from each battery to classify the 8 sets of reusable battery classes, and is connected to the DC common bus. At this time, an internal energy dump was additionally installed using a bidirectional DC/DC converter so that the sum of the internal circulation currents became

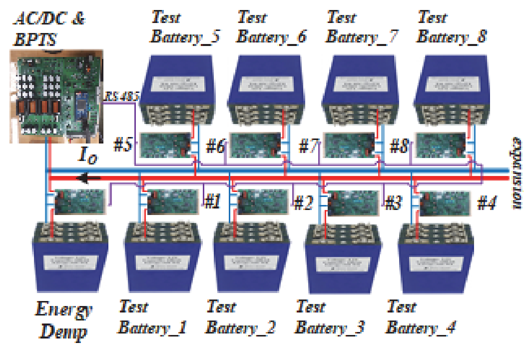

Fig. 7 Configuration of propose system

zero so that the battery charge/discharge test could be performed without external energy supply.

Therefore, this system has a structure that can be used to minimize the operation of the AC/DC converter for energy charging during the reusable battery charge/discharge test. In addition, during the reusable battery charging/discharging test, the operation such as the charging/discharging command value of each converter and the collection of the internal impedance of the battery measured by each converter is managed through RS485 Modbus in the BTPS in the AC/DC converter.

The DC/DC converter composing the system in Fig. 7 can be considered either a step-up /down-type bi-directional converter as shown in Fig. 8(a) or a step-up or step-down type bi-directional converter as shown in Fig. 8(b) from the battery side.

A step-up/down-type bidirectional converter as shown in Fig. 8(a) can be used as a step-up converter regardless of input/output definition, and there is no limit to the input voltage operating range. However, there are

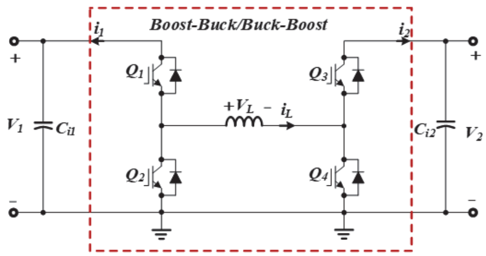

(a) Step-up/down-type bidirectional converter

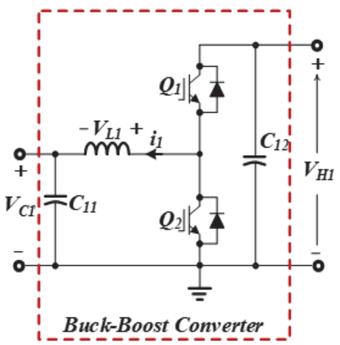

(b) Step-up or step-down type bidirectional converter

Fig. 8 Bidirectional converter topology for battery charging and discharging

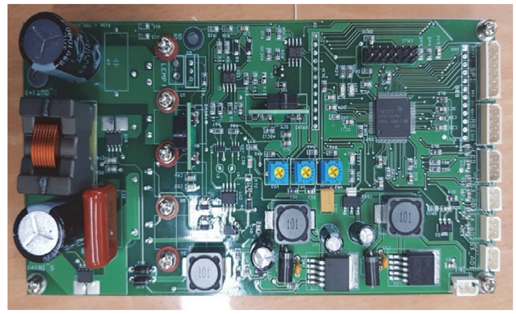

Fig. 9 Bidirectional converter prototype for battery charging and discharging

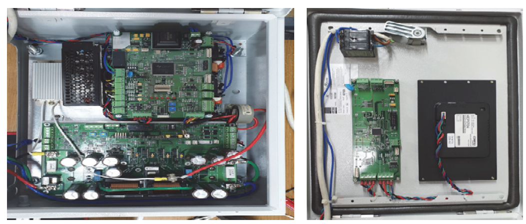

Fig. 10 AC/DC converter and BPTS prototype

disadvantages in terms of high efficiency and system cost due to conduction of two switch elements in the current conduction loop.

On the other hand, the step-up or step-down type bidirectional converter as shown in Fig. 8(b) can only be used as a step-up or step-down converter according to the input/output definition, and the input voltage operating range is limited. However, the conduction of one switch element in the current conduction loop has advantages in terms of high efficiency and unit cost.

Therefore, in this paper, a charging/discharging prototype was manufactured as shown in Fig. 9 by adopting the converter topology as shown in Fig. 8(a). In the manufactured bidirectional DC/D C converter prototype, the DC common bus was set to 48 [V] and the chargeable/discharged voltage was defined as up to 48 [V] to design the system. TI's TMS320F027, a low-cost DSP, was used as the communication and charge/discharge controller.

Fig. 10 shows the AC/DC converter and BTPS prototype. TI's TMS320F335 was used for communication and operation of each converter, and an external memory was installed for data management.

3.2 Experimental results

Fig. 11 is the waveform of the experimental

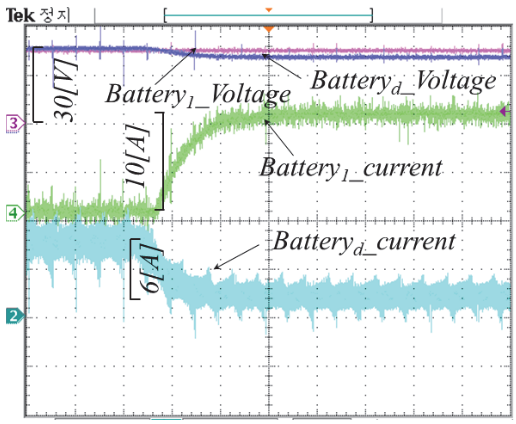

Fig. 11 Operation characteristic waveform of DC/DC converter

result of setting the charge/discharge current to 10 [A] in the battery test system using circulating power between batteries and operating it. It can be seen that the DC/DC converter of Battery 1 is discharging at 10 [A], and the DC/DC converter for Energy Demp is charged at 6 [A], which is the difference between the charging and discharging currents of 8 test batteries.

Fig. 12 is a waveform analysis of the characteristics of the battery during the charging process for the reuse battery test. For waveform analysis, data on average current, voltage, and power were acquired and analyzed in units of 1 second of data log.

Fig. 12(a) shows the current waveform when charging at 13.7[A] with the charging current of 0.5[C]. In order to shorten the charging time, the charging method is not CV control, but CC control, and as shown in the figure, it is charged with a constant current.

Fig. 12(b) shows the charging voltage waveform. As shown in the figure, when the

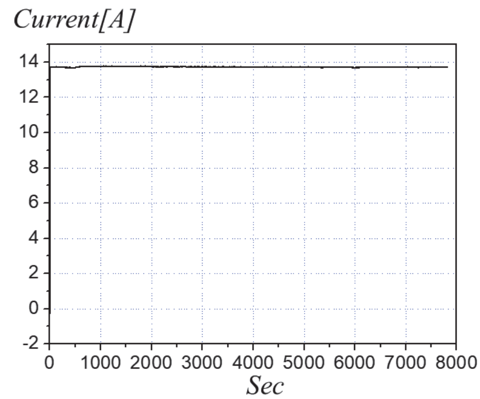

(a) Charging current characteristics

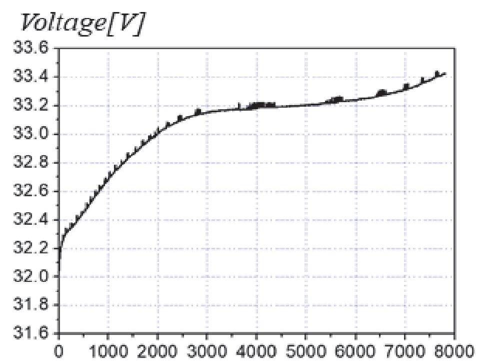

(b) Charging voltage characteristics

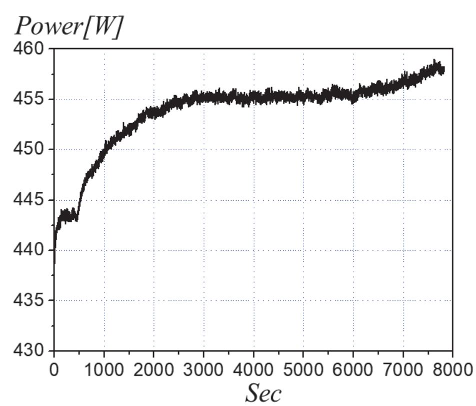

(c) Charging power characteristics

Fig. 12 Battery charge characteristics Waveform

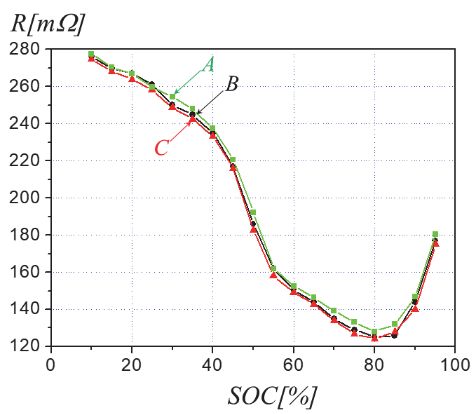

Fig. 13 Characteristics of internal resistance value variation according to the amount of charge

amount of charge is small or large, it can be seen that the voltage slope with respect to the charging current is large, and when the amount of charge is 50[%], the voltage slope is very small.

Therefore, it can be seen that there is a difficulty in detecting the amount of charge by voltage. Fig. 12(c) shows the charging power waveform. As shown in the figure, it can be seen that the average charging power is about 455 [W].

Fig. 13 is the result of detecting the DC equivalent resistance inside the battery while charging under the conditions of Fig. 12. As shown in the figure, it can be seen that the internal resistance of the three test batteries decreases with charging, and its value increases when charging is completed.

Table 2 shows the similarity of each battery when classifying batteries according to Equation (8) according to the similarity of a series of internal resistances measured during the charging process in this paper. As a result of the similarity analysis in Table 2, it was found that the similarity between batteries 1 and 2 was excellent. This similarity analysis technique is considered to be useful when the number of recycled batteries to be tested is large.

Table 2. Battery similarity

	Battery A	*Battery C*
Battery B	*0.66 [%]*	*1.46 [%]*
Battery C	*1.04 [%]*	

4. Conclusion

In this paper, the battery equivalent circuit was analyzed based on the Randles model to analyze the characteristics of the reused battery, and the DCIR method was used for practical measurement of the battery internal impedance of the equivalent circuit. In order to minimize the power consumption during the full charge/discharge test, a charging / discharging system using the circulating power between the batteries sharing the DC-Bus was proposed. In addition, a normalized similarity function suitable for battery characteristics was proposed as a similarity function for classification of recycled batteries using a series of DCIR data measured in a full charge/discharge system. As a result of the experiment to prove the validity of the proposed system and reusable battery classification, it was possible to verify that the proposed topology and classification method are valid.

References

[1] H. D. Lee, O. T. Lim, "Policy Suggestion for Fostering the Industry of Using End of Life EV Batteries," Trans. of the Korean Hydrogen and New Energy Society, Vol. 32, No. 4, pp. 263~270, 2021.

[2] A. Guha and A. Patra, "State of health estimation of lithium ion batteries using capacity fade and internal resistance growth models," IEEE Transaction on Transportation Electrification, Vol. 4, pp. 135-146, 2018.

[3] D. Liu, J. Zhou, H. Liao, Y. Peng, and X. Peng, "A health indicator extraction and optimization framework for lithium ion battery degradation modeling and prognostics," IEEE Transactions on Systems, Man, and Cybernetics: Systems, Vol. 45, pp. 915-928, 2015.

[4] J. Lee and M. F. Pecht, "Reduction of litium ion battery qualificatrion time based on prognostics and health management," IEEE Transactions on Industrial Electronics, Vol. 66, pp. 7310-7315, 2019.

[5] J. Qi et al., "A preventive approach for solving battery imbalance issue by using a bidirectional multiple-input ćuk converter working in DCVM," IEEE Transactions on Industrial Electronics, Vol. 64, pp. 7780-7789, 2017.

[6] V. Agarwal, K. Uthaichana, R. A. Decarlo, L. H. Tsoukalas, "Development and validation of a battery model useful for discharging and charging power control and lifetime estimation," IEEE Trans. Energy. Convers., Vol. 25, No. 3, pp. 821-835.

[7] J.-H. Kim, S.-J. Lee, J.-M. Lee, and B. H. Cho, "A New Direct Current Internal Resistance and State of Charge Relationship for the Li-Ion Battery Pulse Power Estimation," in Proc. of IEEE Int. Conf. Power Electron., pp. 1173-1178, 2007.

[8] M. Uno and K. Tanaka, "Single-switch cell voltage equalizer using multistacked buck–boost converters operating in discontinuous conduction mode for series-connected energy storage cells," IEEE Trans. Veh. Technol., vol. 60, no. 8, pp. 3635–3645, Oct. 2011.

[9] F. Cadini, C. Sbarufatti, F. Cancelliere, and M. Giglio, "State-of-life prognosis and diagnosis of lithium-ion batteries by data-driven particle filters," Applied Energy, Vol. 235, pp. 661-672, 2019.

[10] M. Einhorn, W. Roessler, and J. Fleig, "Improved performance of serially connected li-ion batteries with active cell balancing in electric vehicles," IEEE Trans. Vehicular Tech., vol. 60, no. 99, pp. 2448-2457, May. 2011.

(Manuscript received November 06, 2021;
revised November 27, 2021; accepted December 01, 2021)